HHS Public Access

Author manuscript

AJR Am J Roentgenol. Author manuscript; available in PMC 2017 February 01.

Published in final edited form as:

AJR Am J Roentgenol. 2016 February ; 206(2): 301–306. doi:10.2214/AJR.15.14374.

Appearance and Frequency of Gas Interface Artifacts Involving Small Bowel on Rapid-Voltage-Switching Dual-Energy CT Iodine-Density Images

En-Haw Wu[1], **So Yeon Kim**[2], **Z. Jane Wang**[3], **Wei-Chou Chang**[4], **Li-Qin Zhao**[5], and **Benjamin M. Yeh**[3]

[1]Department of Medical Imaging and Intervention, Chang Gung Memorial Hospital, Linkou and Chang Gung University College of Medicine, Taoyuan County, Taiwan

[2]Department of Radiology and Research Institute of Radiology, Asan Medical Center, University of Ulsan College of Medicine, Seoul, Korea

[3]Department of Radiology and Biomedical Imaging, University of California San Francisco, 505 Parnassus Ave, San Francisco, CA 94143-0628

[4]Tri-Service General Hospital and National Defense Medical Center, Taipei, Taiwan

[5]Department of Radiology, Beijing Friendship Hospital, Capital Medical University, Beijing, China

Abstract

OBJECTIVE—The purpose of this study is to describe the appearance and frequency of gas interface artifacts in the jejunum that may mimic severe bowel disease on iodine-density images generated from rapid-voltage-switching dual-energy CT (DECT) scans.

MATERIALS AND METHODS—Two readers retrospectively reviewed 108 consecutive abdominal rapid-voltage-switching DECT scans to record the presence of image artifacts in jejunal segments with different degrees of gaseous luminal filling, classified as full, partial, or absent. Readers viewed iodine-density images and corresponding 140-kVp and 65-keV virtual monochromatic images and classified the jejunal artifacts on iodine-density images as pseudostratified appearance of the bowel wall, pseudopneumatosis, pseudohyperenhancement, or pseudohypoenhancement. We correlated the presence of the artifacts with clinical features suggesting bowel disease.

RESULTS—Image artifacts were found in 91 of 108 scans (84.3%), appeared in 148 of 265 jejunal segments (55.8%), and included each type except for pseudohypoenhancement. Artifacts occurred exclusively when gas was present in the bowel lumen and were seen in 59 of 59 (100%) fully gas-distended segments, 89 of 98 (90.8%) partially gas-distended segments, and none of 108 gas-absent segments ($p < 0.0001$). In fully and partially gas-distended jejunal segments ($n = 157$), 148 (94.3%) segments had two or more artifacts. None of the patients was found to have clinical bowel-related injury on follow-up of medical records.

Address correspondence to B. M. Yeh (Ben.Yeh@ucsf.edu).

Based on a presentation at the Radiological Society of North America 2014 annual meeting, Chicago, IL.

CONCLUSION—Pseudostratified appearance, pseudopneumatosis, and pseudohyperenhancement, but not pseudohypoenhancement, artifacts are common in gas-filled jejunal segments on iodine-density images generated from rapid-voltage-switching DECT scans and are not seen in the corresponding 140-kVp or 65-keV images. Knowledge of the appearance of such iodine-density image artifacts will avoid potential examination interpretation pitfalls.

Keywords

artifact; DECT; dual-energy CT; jejunum; small bowel

Dual-energy CT (DECT) is an increasingly used technique that provides substantial capabilities compared with conventional CT. One of the transformative benefits of DECT is its ability to distinguish between materials according to their known relative attenuation of two different x-ray spectra [1–3]. Compared with water, soft tissue, and calcium, materials that contain iodine show a high difference in x-ray attenuation when imaged at 80 kVp versus 140 kVp, and this property allows two- or three-material decomposition software to generate iodine-density images from IV contrast-enhanced DECT scans [1–4]. Iodine-density images highlight differences in contrast material distribution at the time of imaging and are useful in imaging solid organs for the detection of subtle hypervascular or hypovascular liver lesions, enhancing renal tumors, endoleaks from endovascular repairs, pancreatic masses, and gastrointestinal bleeding [2, 5–10]. Similarly, iodine-density images generated from DECT scans may be helpful to highlight abnormalities of bowel perfusion, such as to help detect nonenhancement of the bowel wall in bowel ischemia [11], but few data have been published on the use of DECT for bowel imaging. Similarly, there is a paucity of published descriptions of artifacts that are specific to DECT [12].

At routine abdominal readouts of rapid-voltage-switching DECT scans, we encountered iodine-density image artifacts within the bowel at gas interfaces that resembled disease involving the bowel. These artifacts have a striking appearance, but, to our knowledge, have not been previously described. Therefore, we conducted a study to determine the frequency and appearance of these artifacts in relation to gas interfaces in the bowel on clinical rapid-voltage-switching DECT images. In addition, we performed a CT phantom experiment to study these artifacts.

Materials and Methods

Our study was approved by the University of California San Francisco institutional review board and was compliant with HIPAA policy.

Patients

We retrospectively identified 108 consecutive abdominal rapid-voltage-switching DECT studies obtained of 108 unique patients (56 men and 52 women; mean [± SD] age, 59.1 ± 14.8 years) from August 2013 through February 2014. The indications for the CT scans were screening or follow-up for tumor (n = 77), abdominal pain (n = 20), and other (n = 11). One author reviewed the electronic medical records, including imaging reports and clinic notes, to record the presence or absence of bowel disease.

Dual-Energy CT

DECT scans were performed on a rapid-voltage-switching DECT scanner (Discovery CT750 HD, GE Healthcare). All patients were instructed to drink 800 mL of tap water within 1 hour before imaging. No positive oral contrast agent was given. For 78 patients, DECT of the abdomen and pelvis was performed in the portal venous phase using the gemstone spectral imaging mode 80 seconds after the initiation of an IV injection of 150 mL of iohexol (Omnipaque 350, GE Healthcare) with a 50-mL saline flush delivered at 3 mL/s. For the other 30 patients, a dynamic contrast-enhanced abdominal scan was obtained after injection of 120 mL of iohexol with a 50-mL saline flush delivered at 4–5 mL/s, with scan delays determined on the basis of a timing bolus protocol. The dual-energy gemstone spectral imaging mode scan was obtained only for the late arterial phase (scan delay of 30–55 seconds after initiation of contrast injection, depending on the results of the timing bolus). The timing bolus used a 30-mL bolus of iohexol with a 50-mL saline flush.

A limitation of the rapid-voltage-switching DECT scanner is that it does not provide automated exposure modulation for dual-energy scans. However, it does provide an assortment of abdominal gemstone spectral imaging presets that each delivers a certain volumetric CT dose index ($CTDI_{vol}$; range, 8.9–34.4 mGy). Therefore, for each rapid-voltage-switching DECT scan, we chose the abdominal gemstone spectral imaging preset that would deliver a $CTDI_{vol}$ similar to that of a conventional CT scan. The $CTDI_{vol}$ for a conventional CT scan was determined by obtaining a scout topogram and then protocoling (but not scanning) with the following parameters: 40% adaptive statistical iterative reconstruction, noise index of 40.5, slice thickness of 1.25 mm, pitch of 1.375, and 120 kVp. The $CTDI_{vol}$ was noted, and then the abdominal gemstone spectral imaging setting with the most similar $CTDI_{vol}$ was chosen for the rapid-voltage-switching DECT scan. If the $CTDI_{vol}$ was less than 7.5 mGy, then a gemstone spectral imaging mode scan was not obtained because the radiation dose would be substantially higher than that of a conventional CT scan, and those scans were not included in our study.

CT Phantom and Imaging

A water-filled elliptical abdominal CT phantom, measuring approximately 32 × 27 cm in cross-section and 20 cm in length, was cast from the abdomen of a 70-kg male volunteer. The walls of the phantom were made of polyethylene, which has a CT number approximating that of fat. Two sub-compartments of the phantom were filled with 8 mg I/mL iohexol in water to simulate enhanced kidneys, and one subcompartment filled with 10 mg I/mL iohexol in water to simulate the spine. This phantom was fixed to the CT table with tape. To simulate the jejunum, polyethylene corrugated tubing (rebreathing circuit REF: 1610, Hudson RCI-Teleflex Medical) measuring 130 cm in length and with a volume of 400 mL was placed into the water-filled CT phantom. The corrugated tubing had rigid maximal and minimal diameters of 2.4 cm and 1.8 cm, respectively, and was filled with 200 mL of water. The phantom was scanned using the same CT scanner and scan parameters as for the patients. As per the method described already, the gemstone spectral imaging preset that delivered a $CTDI_{vol}$ of 8.9 mGy was used. Iodine-density, 140-kVp, and 65-keV virtual monochromatic images were obtained in the same manner as for the patients. Then the water in the jejunal phantom tubing was removed and replaced with 200 mL of 5 mg I/mL iohexol

to simulate the presence of oral contrast material, and the phantom was rescanned with the same parameters.

Clinical Findings

One of the authors who was not involved in the image analysis investigated clinical features of the patients that were possibly associated with bowel pathologic abnormalities on our electronic medical record system.

Imaging Evaluation

Two readers, each with over 5 years of abdominal imaging subspecialty experience, evaluated all DECT scans in consensus without knowledge of the patients' clinical history. Images were viewed on the Advantage for Windows thin client server (GE Healthcare). For each scan, readers viewed jejunal segments in the left upper quadrant on 140-kVp and 65-keV virtual monochromatic images to classify jejunal segments according to the degrees of gaseous intraluminal filling: fully gas-distended, partially gas-distended, and absent gas (Fig. 1). Fully gas-distended was defined as filling of the lumen with gas without an appreciable gas-fluid level. Partially gas-distended was defined as filling of the lumen with gas and fluid, with the presence of a visible fluid-fluid level. Absent gas was defined as either collapsed bowel or bowel filled with fluid without visible gas. A representative segment of jejunum for each of the three categories in each patient was selected. If only one or two categories of jejunum was found, then only representative segments from those one or two categories were selected for evaluation.

Then reviewers viewed the identified jejunal segments on the corresponding iodine-density images—also called "iodine(water)" images—to evaluate for the presence or absence of image artifacts involving those bowel segments. Image artifacts were considered to be present if a similar appearance of the bowel wall was not seen on the 140-kVp or 65-keV virtual monochromatic images. If an image artifact was present, the artifact was classified as follows: pseudostratified bowel wall artifact, defined as three or more thin alternating parallel bands of bright and dark signal involving and parallel to the bowel wall; pseudopneumatosis, defined as irregular small beaded signal voids adjacent to bowel mucosa; pseudohyperenhancement, defined as intense high signal of the bowel folds brighter than that of contrast material in the blood vessels (Fig. 2); and pseudohypoenhancment, defined as distinctly lower apparent enhancement of the bowel folds on iodine-density images in comparison what would be expected when viewing the 140-kVp and 65-keV images [13, 14]. The locations of the artifacts relative to the bowel wall were recorded. Similar assessment of the rapid-voltage-switching DECT phantom scans were made as for the patient scans.

Statistical Analysis

Statistical analysis was performed using SPSS software (version 22.0.0.0, IBM). The frequency of finding each type of artifact in each class of jejunal bowel segment according to the degrees of gaseous intraluminal filling were compared by chi-square analysis. Bivariate correlation analysis was performed to determine the associations among three

different types of artifact. A p value less than 0.05 was considered to be statistically significant.

Results

We evaluated a total of 265 representative jejunal segments (59 fully gas-distended, 98 partially gas-distended, and 108 absent gas). All three degrees of jejunal gas distention were seen in 57 patients, and only two and one degree of distention were seen in 43 and eight patients, respectively. Bowel artifacts were observed in 148 (55.8%) segments and were seen in 91 of 108 scans (84.3%). No interface artifacts were seen on the 140-kVp or 65-keV virtual monochromatic images. The artifacts were seen exclusively in jejunal segments containing gas (Table 1), and appeared in 59 of 59 (100%) fully gas-distended, 89 of 98 (90.8%) partially gas-distended (Fig. 3), and none of 108 gas-absent jejunal segments. In fully and partially gas-distended segments (n = 157), 148 (94.3%) segments had two or more artifacts (Table 2) with 110 segments showing pseudostratified bowel wall, 30 showing pseudopneumatosis, and 138 showing pseudohyperenhancement. None of the segments was found to show pseudohypoenhancement of the bowel wall. None of the patients was found to have bowel-related injury on review of follow-up medical records.

The presence of pseudostratified bowel wall and pseudohyperenhancement were statistically significantly associated (r = 0.65; $p < 0.05$). Pseudostratified artifact was negatively associated with pseudopneumatosis ($r = -0.18$; $p < 0.05$) (Table 3).

In the CT phantom (Fig. 4), pseudohyperenhancement, pseudopneumatosis, and pseudostratified iodine-density image artifacts were seen exclusively in phantom bowel segments containing gas. Pseudohyperenhancement of the bowel wall was seen despite the absence of contrast material in the bowel wall. The artifacts were present on the iodine-density images at gas interfaces regardless of whether water or oral contrast agent was in the phantom bowel lumen.

Discussion

We found that gas interface artifacts are frequently seen in the jejunum on iodine-density images generated from routine rapid-voltage-switching DECT studies. The artifacts may appear as pseudohyperenhancement, pseudopneumatosis, or pseudostratified appearance. The artifacts are seen only when some gas distention of the bowel lumen is present and are absent in collapsed segments or segments with complete filling with fluid. No corresponding jejunal abnormality was seen on the 140-kVp or 65-keV virtual monochromatic images. The image artifacts seen in patients are readily reproduced in a CT phantom that contains gas in phantom bowel segments. Notably, the appearance of vivid hyperenhancement may be seen on iodine-density images, even in the absence of contrast material, as shown in our CT phantom test.

Our findings contribute to the growing body of knowledge regarding the interpretation of DECT images. A major benefit of DECT in the abdomen is for highlighting iodine contrast signal. Iodine-density images improve the conspicuity and detection of hyper- or hypovascular lesions in the liver or pancreas. Furthermore, DECT can substantially reduce

artifacts, such as metal spray artifact, seen on conventional CT [15, 16]. Prior publications have shown that DECT may help identify areas of bowel hypoenhancement [11]. Our findings build on this prior work by showing that that pseudohypoenhancement does not appear to occur in iodine-density maps. We also add to the literature by describing three bowel-related artifacts, including their characteristic appearances and locations at gas, fluid, and soft-tissue interfaces, that can mimic clinically relevant bowel findings on iodine-density images. Familiarization of radiologists with these prevalent image artifacts is important as an increasing number of radiologists adopt DECT in clinical practice.

In consultation with GE Healthcare, the causes of the gas-tissue interface artifacts, including the pseudohyperenhancement, pseudopneumatosis, and pseudostratified bowel wall appearances, are not clear. Because the artifacts are seen only on the iodine-density images rather than the virtual monochromatic images, the artifacts are not likely due to edge-enhancement filtering or 80–140 kVp signal misregistration because such errors should affect all images and not just the iodine-density images. The physics theory of the material decomposition calculation for iodine-density imaging indicates that air and the surrounding soft tissue or water have similar density values, even though there is a large attenuation difference in the source images. This makes it difficult to observe these small attenuation differences and results in the gas-tissue interface artifact being seen in only the iodine-density images (Madhav P, GE Healthcare, written communication, August 18, 2014). GE Healthcare is currently investigating approaches to overcome these limitations in the iodine material density images (Madhav P, GE Healthcare, written communication, August 18, 2014). Until the cause of artifacts are resolved, it will be critical for radiologists to recognize that such gas-tissue interface artifacts are highly common and distinctive and should not be mistaken for bowel disease.

Our study focused on the bowel because of the similarity of these artifacts to commonly sought CT findings of severe bowel disease. However, at daily readout sessions, we also observe gas-tissue interface artifacts in other gas-containing segments of the bowel, such as the colon, stomach, and ileum, and also along the gas interface with skin, airway walls, and at the boundary between the lung and the mediastinum or chest wall (Fig. 3). The frequency of such artifacts in those locations is beyond the scope of our current investigation.

Our study has several limitations. First, our study is retrospective, and the rapid-voltage-switching DECT studies were obtained primarily for staging or follow-up of abdominal tumor or were obtained for non-bowel indications. None of the examinations was obtained specifically for evaluation of the gastrointestinal tract. However, our study population reflects those who undergo DECT scans in a tertiary care institution. Second, our observations are based on the datasets from the two-material decomposition postprocessing technique from the rapid-voltage-switching single-source CT platform. We did not study images from the other types of DECT scanners, such as the dual-source, sandwich-detector, twin-beam, or rotate-rotate platforms, because these types of machines are not available in our institution. Further studies would be needed to assess for the presence or absence and relative severity of gas interface artifacts between different DECT platforms. Third, our study was limited to the evaluation of the jejunum because the ileum and whole colon were not included in the scanned region for many of our patients who underwent only abdominal

scans. Fourth, our study was focused on routine abdomen and pelvis CT scans, not dedicated CT enterography examinations in which close evaluation of small bowel is of highest concern. On the basis of our findings, future studies on the use of DECT for CT enterography are needed to assess for potential bowel-related artifacts.

In conclusion, jejunal gas interface artifacts are frequently seen on iodine-density images generated from rapid-switching DECT scans. Pseudostratified appearance, pseudopneumatosis, and pseudohyperenhancement artifacts were common in the jejunum on iodine-density images, but pseudohypoenhancement was not seen. These artifacts are significantly associated with the degree of gas distention of the jejunum and occur at the interface between gas and soft tissue or fluid. Radiologists evaluating iodine-density images generated from rapid-voltage-switching DECT scans should be aware of the common appearances of gas interface artifacts. Reference to the 140-kVp or 65-keV virtual monochromatic contrast-enhanced images can help avoid mistaking artifacts as true bowel pathologic abnormalities. Further investigation will be required to confirm the causes of these artifacts and to reduce them in future generations of the rapid-voltage-switching DECT scanner.

Acknowledgments

Z. J. Wang is a shareholder of Nextrast, Inc. B. M. Yeh receives research grants from GE Healthcare and book royalties from Oxford University Press and is a shareholder of Nextrast, Inc.

Supported in part by grants 1R41DK104580 and 1R01EB015476 from the U.S. National Institutes of Health.

References

1. Coursey CA, Nelson RC, Boll DT, et al. Dual-energy multidetector CT: how does it work, what can it tell us, and when can we use it in abdominopelvic imaging? RadioGraphics. 2010; 30:1037–1055. [PubMed: 20631367]
2. Morgan DE. Dual-energy CT of the abdomen. Abdom Imaging. 2014; 39:108–134. [PubMed: 24072382]
3. Marin D, Boll DT, Mileto A, Nelson RC. State of the art: dual-energy CT of the abdomen. Radiology. 2014; 271:327–342. [PubMed: 24761954]
4. Aran S, Shaqdan KW, Abujudeh HH. Dual-energy computed tomography (DECT) in emergency radiology: basic principles, techniques, and limitations. Emerg Radiol. 2014; 21:391–405. [PubMed: 24676736]
5. Aran S, Daftari Besheli L, Karcaaltincaba M, Gupta R, Flores EJ, Abujudeh HH. Applications of dual-energy CT in emergency radiology. AJR. 2014; 202:W314–W324. web. [PubMed: 24660729]
6. Yeh BM, Shepherd JA, Wang ZJ, Teh HS, Hartman RP, Prevrhal S. Dual-energy and low-kVp CT in the abdomen. AJR. 2009; 193:47–54. [PubMed: 19542394]
7. Graser A, Johnson TR, Chandarana H, Macari M. Dual energy CT: preliminary observations and potential clinical applications in the abdomen. Eur Radiol. 2009; 19:13–23. [PubMed: 18677487]
8. Patel BN, Thomas JV, Lockhart ME, Berland LL, Morgan DE. Single-source dual-energy spectral multidetector CT of pancreatic adenocarcinoma: optimization of energy level viewing significantly increases lesion contrast. Clin Radiol. 2013; 68:148–154. [PubMed: 22889459]
9. Heye T, Nelson RC, Ho LM, Marin D, Boll DT. Dual-energy CT applications in the abdomen. AJR. 2012; 199(suppl 5):S64–S70. [PubMed: 23097169]
10. Mileto A, Nelson RC, Samei E, et al. Impact of dual-energy multi-detector row CT with virtual monochromatic imaging on renal cyst pseudoenhancement: in vitro and in vivo study. Radiology. 2014; 272:767–776. [PubMed: 24844472]

11. Potretzke TA, Brace CL, Lubner MG, Sampson LA, Willey BJ, Lee FT Jr. Early small-bowel ischemia: dual-energy CT improves conspicuity compared with conventional CT in a swine model. Radiology. 2015; 275:119–126. [PubMed: 25426772]
12. Fraioli F, Ciarlo G, Anzidei M. Dual-energy CT: too many artifacts? AJR. 2011; 197:W783. web. [PubMed: 21940555]
13. Macari M, Megibow AJ, Balthazar EJ. A pattern approach to the abnormal small bowel: observations at MDCT and CT enterography. AJR. 2007; 188:1344–1355. [PubMed: 17449781]
14. Macari M, Balthazar EJ. CT of bowel wall thickening: significance and pitfalls of interpretation. AJR. 2001; 176:1105–1116. [PubMed: 11312162]
15. Han SC, Chung YE, Lee YH, Park KK, Kim MJ, Kim KW. Metal artifact reduction software used with abdominopelvic dual-energy CT of patients with metal hip prostheses: assessment of image quality and clinical feasibility. AJR. 2014; 203:788–795. [PubMed: 25247944]
16. Mangold S, Gatidis S, Luz O, et al. Single-source dual-energy computed tomography: use of monoenergetic extrapolation for a reduction of metal artifacts. Invest Radiol. 2014; 49:788–793. [PubMed: 24979325]

Fig. 1. Three representative types of jejunal segments

A, 83-year-old woman with fully gas-distended segment. Jejunum is fully distended with gas without substantial fluid or solid material in bowel lumen.

B, 73-year-old woman with partially gas-distended segment. Jejunum shows distention with gas and fluid, with gas-fluid levels seen in bowel.

C, 46-year-old man with absent gas segment. Jejunum does not contain substantial gas in lumen and may be collapsed or fluid-containing.

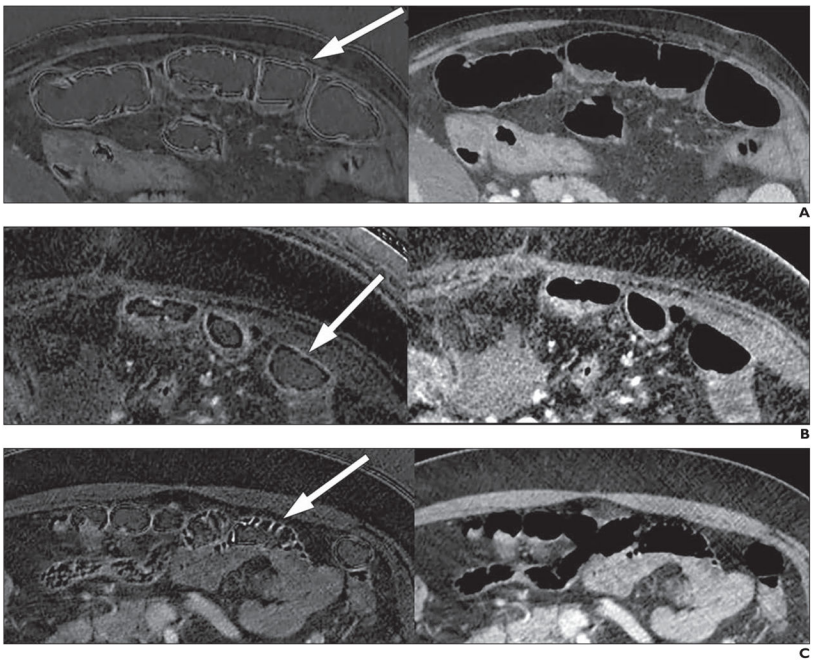

Fig. 2. Interface artifact on dual-energy CT iodine-density images and 65-keV images

A, 55-year-old man with pseudostratified bowel wall artifact. Three or more thin alternating parallel bands of bright and dark signal (*arrow*) appear on iodine-density image (*left*), but are not seen on 65-keV image (*right*).

B, 63-year-old woman with pseudopneumatosis artifact. Iodine image (*left*) shows irregular small beaded signal voids adjacent to bowel mucosa (*arrow*). Image obtained at 65 keV is shown on right.

C, 49-year-old man with pseudohyperenhancement artifact. Iodine image (*left*) shows intense high signal of bowel folds (*arrow*) that is brighter than that of visible blood vessels. Image obtained at 65 keV is shown on right.

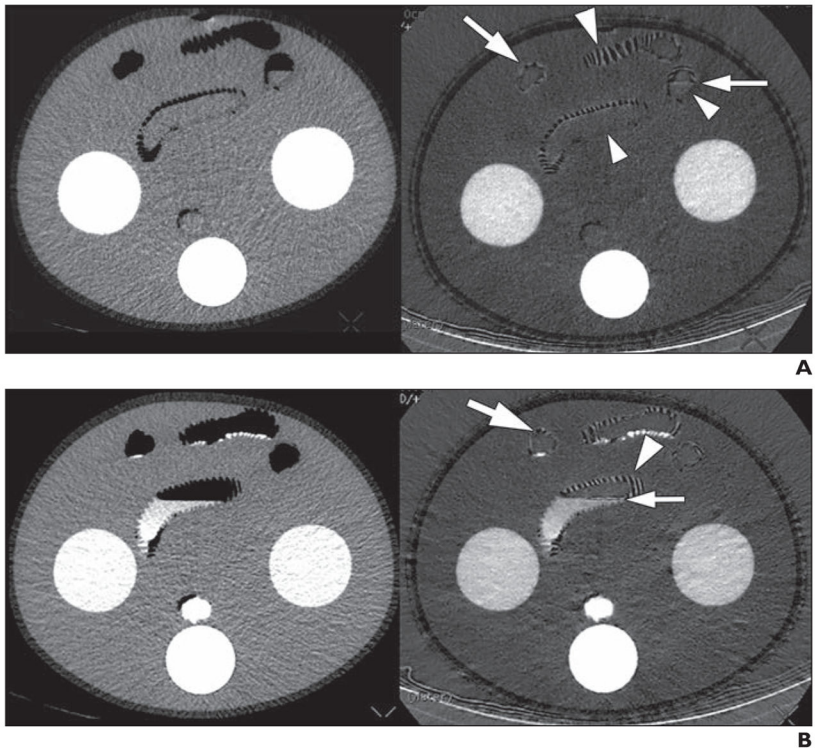

Fig. 3. Dual-energy CT gas interface artifact in phantom

A, Phantom imaged without oral contrast material shows artifacts on iodine-density image (*right*), including pseudohyperenhancement (*large arrowhead*), pseudopneumatosis (*large arrow*), and pseudostratified appearance (*small arrow*) at interfaces between air and bowel wall or fluid. No artifact is seen in portions of bowel wall that do not have interface with gas (*small arrowheads*). These artifacts are not seen on corresponding 65-keV image (*left*).

B, Phantom imaged with oral contrast material shows similar findings of artifacts on iodine-density image (*right*) as were seen in phantom without oral contrast material, including pseudohyperenhancement (*large arrowhead*), pseudopneumatosis (*large arrow*), and pseudostratified appearance (*small arrow*) at interfaces between air and bowel wall or fluid. These artifacts are not seen on corresponding 65-keV image (*left*).

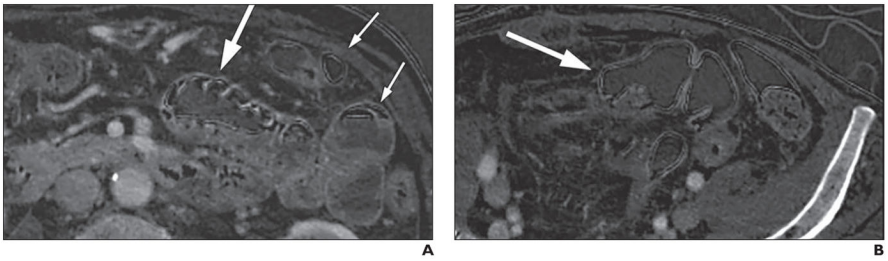

Fig. 4. Examples of iodine-density images of abdomen and pelvis that show gas interface artifacts in nonjejunal structures

A, 57-year-old woman with pseudostratified and pseudohyperenhancement artifacts in partially gas-distended jejunal segment (*large arrow*). Pseudostratified artifact is also seen in gas-distended portion of descending colon (*small arrows*) at gas-bowel and gas-fluid interfaces. Artifact is also seen at gas-skin interface.

B, 71-year-old woman with pseudostratified artifact also in gas-filled sigmoid colon (*arrow*).

TABLE 1

Number of Artifacts by Jejunal Bowel Type on Late Arterial and Venous Phase Images

Bowel Type	Late Arterial Phase Images			Venous Phase Images			Overall Total
	Artifact Present	Artifact Absent	Subtotal	Artifact Present	Artifact Absent	Subtotal	
Full gas	11	0	11	48	0	48	59
Partial gas	19	7	26	70	2	72	98
Absent gas	0	30	30	0	78	78	108
Total	30	37	67	118	80	198	265

Note—$p < 0.05$, chi-square test for presence of artifact between the bowel segments.

TABLE 2

Numbers of Three Types of Artifacts by the Jejunal Bowel Type on Late Arterial and Venous Phase Images

	Late Arterial Phase Images					Venous Phase Images				
Bowel Type	**No. of Artifacts**	**Pseudo-stratified**	**Pseudo-pneumatosis**	**Pseudohyper-enhancement**	**Pseudohypo-enhancement**	**No. of Artifacts**	**Pseudo-stratified**	**Pseudo-pneumatosis**	**Pseudohyper-enhancement**	**Pseudohypo-enhancement**
Full gas[a]	11	3	7	11	0	48	44	7	45	0
Partial gas[a]	26	6	8	16	0	72	57	8	66	0
Absent gas	30	0	0	0	0	78	0	0	0	0
Total	67	9	15	27	0	198	101	15	111	0

[a]More than one type of artifact was identified in each bowel segment.

TABLE 3

Bivariate Correlations Among the Artifacts (n = 265)

Type of Artifact	Pseudostratified	Pseudopneumatosis	Pseudohyperenhancement
Pseudostratified	1	−0.18	0.65
Pseudopneumatosis	−0.18	1	0.34
Pseudohyperenhancement	0.65	0.34	1

Note—Data are r values (correlation coefficients).